CHALMERS

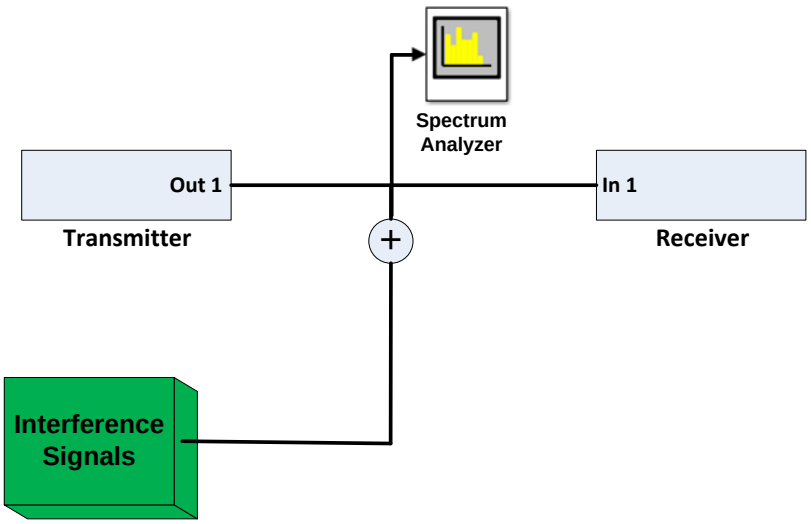

Development of IEEE 802.11p Transceiver in Simulink & Evaluation of the Electromagnetic Interference Effects

DENGZHENG HUANG
RAGAD MAJEED

Report number: EX047/2015
Department of Signals and Systems
Chalmers University of Technology
Göteborg, Sweden 2014
Master's Thesis

Development of IEEE 802.11p Transceiver in Simulink & Evaluation of the Electromagnetic Interference Effects

Dengzheng Huang
Ragad Majeed

Department of Signals and Systems
CHALMERS UNIVERSITY OF TECHNOLOGY
Göteborg, Sweden 2014

Development of IEEE 802.11p Transceiver in Simulink & Evaluation of the Electromagnetic Interference Effects.

DENGZHENG HUANG
RAGAD MAJEED

Department of Signals and Systems
Chalmers Univerisity of Technology
SE-412 96 Göteborg
Sweden
Telephone +46(0)31-772 1000

Göteborg, Sweden 2014

Abstract

Electromagnetic Interference (EMI) always causes operation disruption in any electronic device. Due to the increase of electronic components in cars, the effect of EMI on other safety critical devices has to be analyzed. In this thesis we investigate the effect of EMI on Vehicle to Vehicle (V2V) communication systems, which will enable safety critical applications in the future.

In this thesis, an Institute of Electrical and Electronics Engineers (IEEE) 802.11p transceiver in Simulink is implemented for evaluating the effects of EMI. The model can be used for different scenarios and interference environments, like changing the channels characteristics, adding a simulated channel or even to test with different modulation schemes.

The transceiver implementation consists of three parts, the transmitter, the receiver and the intermediate channel block. The transmitter model generates IEEE 802.11p compliant frames, the intermediate channel block can be used to introduce fading, noise and different interference signals, and the receiver model contains the frame detection, the alignment of the In-phase and Quadrature (IQ) samples, frequency offset correction, and the removal of the preamble and guard signals to recover the transmitted data source.

The simulation model has been verified by comparing the results of the model with and without convolutional encoder and decoder. The simulation results were compared to the theoretical performance results to check the correctness of the model. Different types of interference signals are introduced in the system to calculate packet error rates at different values of signal to noise ratio for each interference signal.

A complete physical layer implementation of IEEE 802.11p has been developed and it can be used to interface with a compatible software defined radio in the future.

Acknowledgements

We would like to thank our examiner Professor Erik Ström for his knowledge and support, and we would also like to thank our advisor Keerthi Nagalapur for his patience and for guiding us all the way through our thesis journey. He explained every problem with patience and provided us with good knowledge which made us go forward and achieve our goal.

Many thanks to our families and parents who helped and supported us although our study with the thesis project.

Finally, we would like to thank our leader Björn Bergqvist at Volvo Cars Corporation for supporting us and being kind and supportive all the time, and also to thank Torbjörn Persson for providing us with the hardware equipment.

Contents

List of Figures

List of Tables

List of Abbreviations

AM Amplitude Modulation

AWGN Additive White Gaussian Noise

BER Bit Error Rate

BPSK Binary Phase Shift Keying

CW Continuous Wave

EMC Electromagnetic Compatibility

EMI Electromagnetic Interferences

FFT Fast Fourier Transform

FM Frequency Modulation

IEEE Institute of Electrical and Electronics Engineers

IFFT Inverse Fast Fourier Transform

ISI Inter Symbol Interference

IQ In-phase and Quadrature

ITS Intelligent Transportation Systems

OFDM Orthogonal Frequency Division Multiplexing

PER Packet Error Rate

PHY Physical layer

PLCP Physical layer Convergence Protocol

PSDU PLCP Service Data Unit

QAM Quadrature Amplitude Modulation

QPSK Quadrature Phase Shift Keying

SIR Signal to Interference Ratio

SNR Signal to Noise Ratio

USRP Universal Software Defined Radio Peripherals

V2V Vehicle To Vehicle

WAVE Wireless Access in Vehicular Environment

1

Introduction

1.1 Background

Vehicular communication has become one of the most active research areas both for industry and academia due to its potential applications ranging from providing safety, applications like traffic efficiency, reduce fuel consumption, emergency vehicle warning, stationary vehicle warning, pre-crash support, hazardous location warning, and signal violation warning. These applications lie within a band centered at 5.9 GHz.

Institute of Electrical and Electronics Engineers (IEEE) 802.11p [1] is the physical layer standard chosen in the Wireless Access in Vehicular Environment (WAVE) architecture. It is an amendment to the well known IEEE 802.11a, which enables applications in fast changing vehicular networks. The European standards is known as the Intelligent Transportation Systems (ITS)-G5.

The car industry has shown a great interest in the research and development of Vehicle To Vehicle (V2V) and therefore Volvo Cars is working on how to improve the communication performance in presence of interference. Volvo Cars would like to set the right requirements for the components that are used for transmitting and receiving messages within the V2V communication standard. It is necessary to investigate the behavior in simulation test environment before these components are built in the car.

This thesis is focused on developing a transceiver model in Simulink/Matlab which is based on baseband processing and adding different types of interference signals; to be able to evaluate the effect of the Electromagnetic interference.

A simulation model in Simulink/Matlab is implemented in this thesis work, and that model is used for testing the reliability of the IEEE 802.11p reception with

different interference signals. The simulated model could be adapted to use and test on real hardware with wired or wireless environment. The preferred hardware setup is Ettus N210, equipped with the recommended daughter boards XCVR2450 with frequency ranges 2.4-2.5 GHz and 4.9-5.9 GHz, and these daughter boards cover the frequency ranges specified for V2V communications.

1.2 Objectives and scope

This thesis work is part of Volvo Cars Corporation's work within the FFI project EMCCOM which is a VINNOVA financed project aiming at developing new Electromagnetic Compatibility (EMC) component requirements suited for digital communication and simple models to predict radio performance degradation. The thesis scope is to investigate different EMC interferences, for instance Continuous Wave (CW), Amplitude Modulation (AM) Wave, Frequency Modulation (FM) Wave and their influence on the communication system in Simulink modeling with IEEE 802.11p.

1.3 Methodology

The work procedure for this thesis work is starting with literature study about the characteristics and specifications of IEEE 802.11p to determine the suitable hardware and software that meet the requirements. The work is based on establishing the simulation model by using Simulink/Matlab modeling and then separating the model into two parts, one for the transmitter and one for the receiver to be deployed on two computers and two Universal Software Defined Radio Peripherals (USRP) devices.

Due to the limitation in the USRP hardware, the model is adapted for only computer simulations and by introducing four interference signals to the transmitted signal. The effect of the interference on the Bit Error Rate (BER) and Packet Error Rate (PER) is evaluated.

1.4 Thesis description

This report comprises of six chapters, Chapter 2 describes the simulated model, and the Orthogonal Frequency Division Multiplexing (OFDM) physical layer of the IEEE 802.11p standard. Chapter 3 describes the transmitter model implementation. In Chapter 4 the receiver model is explained and described. Chapter 5 describes the intermediate block (channel and interferences), and finally Chapter 6 lists the conclusions and suggestions for future work.

2

System Overview

2.1 IEEE 802.11p protocol architecture

The WAVE architecture covers different working layers and the model used in this thesis work is based on the low level layer which is called the physical layer. Figure 2.1 shows where this layer is placed in the standard architecture.

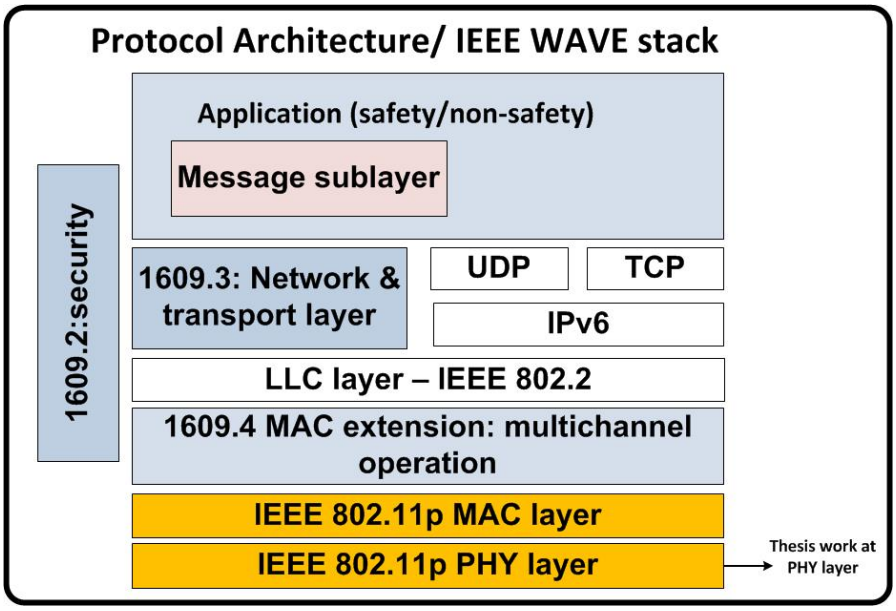

Figure 2.1: IEEE WAVE stack

2.2 System simulation block diagram

Figure 2.2 shows the system overview of the thesis work and each block is implemented in a Simulink/Matlab model which is described in detail in this report. The block diagram shows the transceiver two parts and the intermediate channel. The transmitter generates preamble, SIGNAL and DATA. The intermediate channel in this thesis work consists of the interference signals, which are described in detail in the report. The receiver part contains the most important recovering parts which are frame detection, symbol alignment, frequency offset, channel estimation, decoding, demodulation and descrambling blocks.

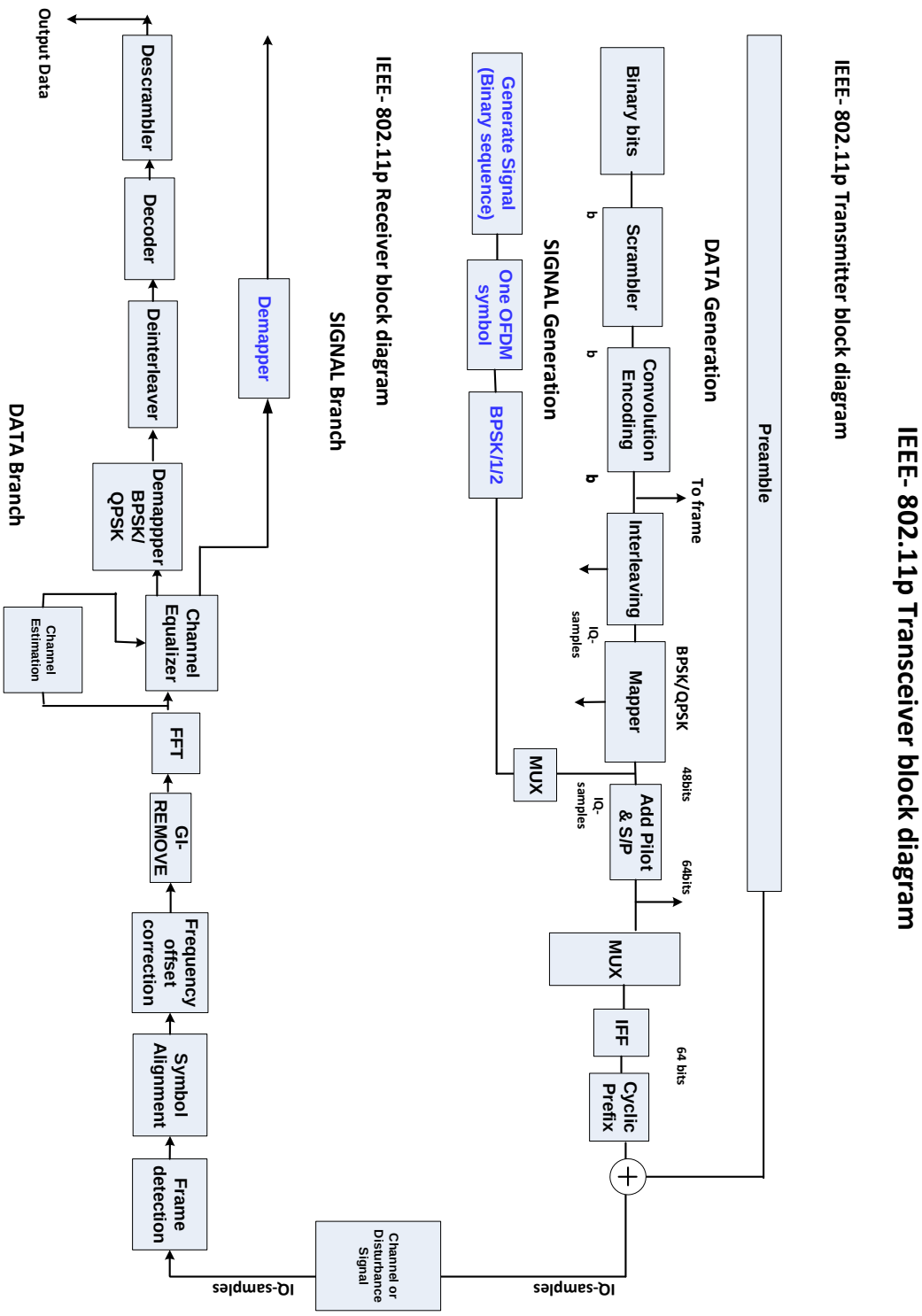

Figure 2.2: Block diagram of the transceiver simulation model

3

The Transmitter

The transmitter part in the model is based on implementing the Physical layer Convergence Protocol (PLCP) frame in Simulink. The PLCP frame consists of three parts, the PLCP Preamble, the SIGNAL, which is one OFDM symbol long, and the DATA part which consist of variable numbers of OFDM symbols [1].

The preamble is the same as in 802.11a and is used for frame detection, timing and frequency synchronization and also for channel estimation.

The PLCP Service Data Unit (PSDU) part for this thesis is a message phrase which consist of 2000 bits. The message phrase is 'Development of IEEE 802.11p Transceiver in Simulink & Evaluation of the Electromagnetic InterferenceDevelopment of IEEE 802.11p Transceiver in Simulink & Evaluation of the Electromagnetic InterferenceDevelopment of IEEE 802.11p Transeiver in Simulin'.

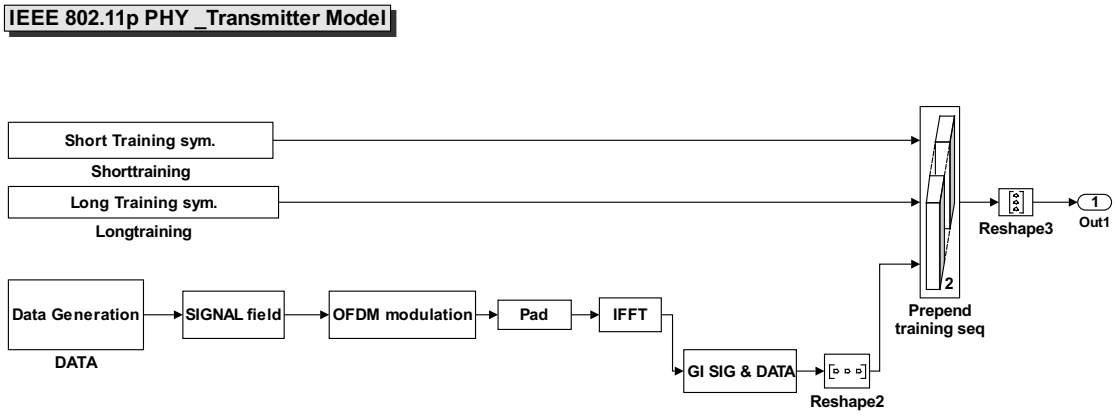

Figure 3.1: Transmitter model in Simulink/Matlab

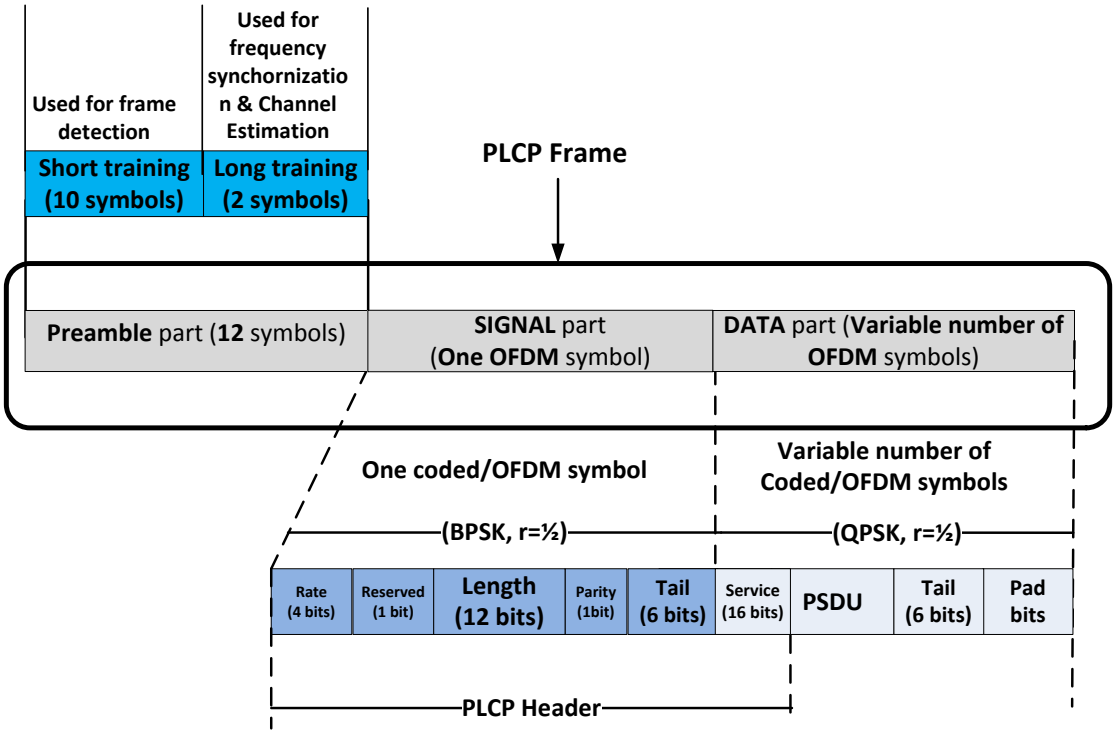

Figure 3.2: PLCP frame contents

Figure 3.2 shows the detailed frame. For 10 MHz channel spacing, the timing related parameters are shown in Table 3.2. The 10 MHz OFDM training structure is shown in Figure 3.3.

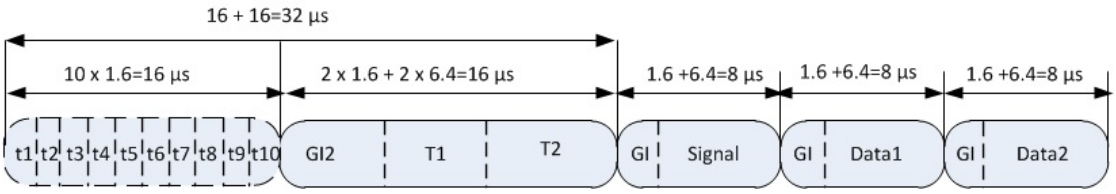

Figure 3.3: The PLCP frame contents

Table 3.1 describes the modulation and coding schemes used in IEEE 802.11p. In the Simulink model, the modulation and coding scheme for the DATA part is Quadrature Phase Shift Keying (QPSK), Coding Rate $R = 1/2$.

Table 3.1: Modulation-dependent parameters

Modulation	Coding rate (R)	Coded bits per subcarrier (N_{BPSC})	Coded bits per OFDM symbol (N_{CBPS})	Data bits per OFDM symbol (N_{DBPS})	Data rate (Mb/s) (10 MHz channel spacing)
BPSK	1/2	1	48	24	3
BPSK	3/4	1	48	36	4.5
QPSK	1/2	2	96	48	6
QPSK	3/4	2	96	72	9
16-QAM	1/2	4	192	96	12
16-QAM	3/4	4	192	144	18
64-QAM	2/3	6	288	192	24
64-QAM	3/4	6	288	216	27

3.1 PLCP preamble

3.1.1 Short training sequence

The short training sequence is given by [1]

SHORTTRAIN = $\sqrt{(13/6)} \times$ [0; 0; 1+1i; 0; 0; 0; -1-1i; 0; 0; 0; 1+1i; 0; 0; 0; -1-1i; 0; 0; 0; -1-1i; 0; 0; 0; 1+1i; 0; 0; 0; 0; 0; 0; 0; -1-1i; 0; 0; 0; -1-1i; 0; 0; 0; 1+1i; 0; 0; 0; 1+1i; 0; 0; 0; 1+1i; 0; 0; 0; 1+1i; 0; 0] .

There are 12 utilized subcarriers out of 52 total subcarriers. The factor $\sqrt{(13/6)}$ is used in order to normalize the average power of the resulting OFDM symbol. After IFFT operation, this sequence results in a periodic waveform, which is used for frame detection and frequency offset correction at the receiver.

Table 3.2: Timing realated parameters of 10 MHz channel spacing

Parameter	Value(10 MHz channel spacing)
N_{SD}: Number of data subcarriers	48
N_{SP}: Number of pilot subcarriers	4
N_{ST}: Number of subcarriers	52 ($N_{SD} + N_{SP}$)
Δ_F: Subcarrier separation	0.15625 MHz (= 10 MHz/64)
T_{FFT}: Inverse Fast Fourier Transform (IFFT) /Fast Fourier Transform (FFT) period	6.4 μs ($1/\Delta_F$)
$T_{PREAMBLE}$: PLCP preamble duration	32 μs ($T_{SHORT} + T_{LONG}$)
T_{SIGNAL}: Duration of the SIGNAL BPSK-OFDM symbol	8 μs ($T_{GI} + T_{FFT}$)
T_{GI}: GI duration	1.6 μs ($T_{FFT}/4$)
T_{GI2}: Training symbol GI duration	3.2 μs ($T_{FFT}/2$)
T_{SYM}: Symbol interval	8 μs ($T_{GI} + T_{FFT}$)
T_{SHORT}: Short training sequence duration	16 μs ($10 \times T_{FFT}/4$)
T_{LONG}: Long training sequence duration	16 μs ($T_{GI2} + 2 \times T_{FFT}$)

3.1.2 Long training sequence

The long training sequence is obtained from [1]

LONGTRAIN = [1; 1; -1; -1; 1; 1; -1; 1; -1; 1; 1; 1; 1; 1; 1; -1; -1; 1; 1; -1; 1; -1; 1; 1; 1; 1; 0; 1; -1; -1; 1; 1; -1; 1; -1; 1; -1; -1; -1; -1; -1; 1; 1; -1; -1; 1; -1; 1; -1; 1; 1; 1; 1].

The long training sequence is used for symbol alignment and channel estimation at the receiver.

3.2 SIGNAL generation

The SIGNAL field contains 4 RATE bits and 12 LENGTH bits, the LENGTH field indicates the length of the data in bytes and the RATE field indicates the modulation and coding scheme for the data. The SIGNAL field is described as in

Figure 3.4. The dark field in Table 3.3 shows the RATE field used in the system.

Table 3.3: Contents of the RATE field for 10 MHz

R1-R4	Rate(Mb/s)(10 MHz channel spacing)
1101	3
1111	4.5
0101	6
0111	9
1001	12
1011	18
0001	24
0011	27

In the designed model, the value in SIGNAL field has 24 bits, bit 0 to 3 stand for the data rate, bit 5 to 16 describe the length of PSDU in numbers of octets.

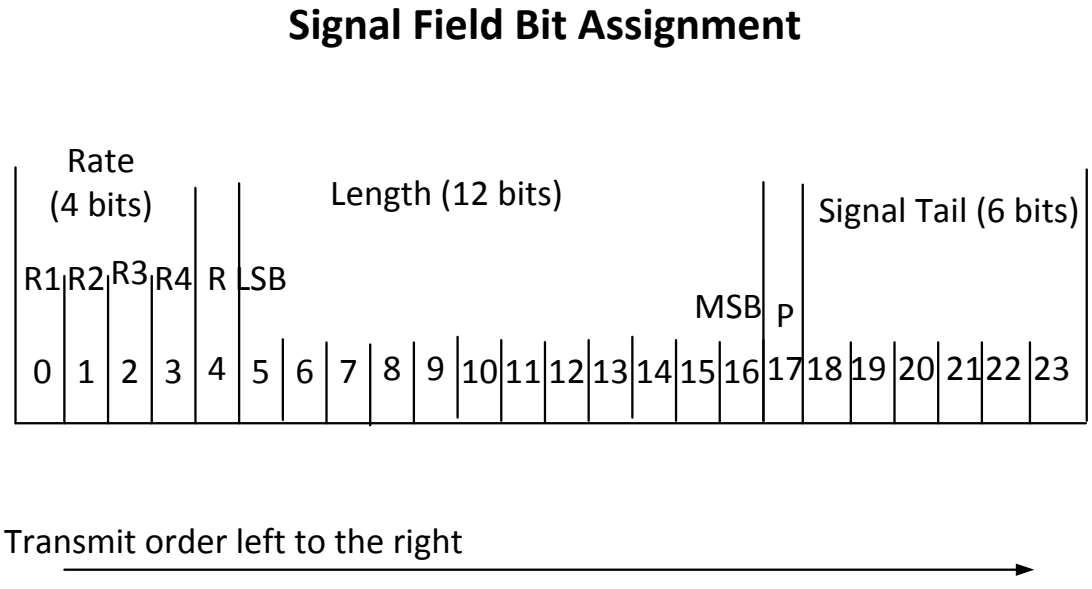

Figure 3.4: SIGNAL field bit assignment

3.3 Data generation

The DATA field is a part of the PLCP frame including 16 bits SERVICE field, of which first 7 are zeros used to retrieve the initial state of the scrambler at the receiver. The PSDU is the information part of 250 bytes (2000 bits). There are 6 zeros of tail bits and 42 zeros of pad bits. The number of pad bits N_{PAD} is calculated by

$$N_{\mathrm{SYM}} = \lceil (16 + 8 \times \mathrm{LENGTH} + 6)/N_{\mathrm{DBPS}} \rceil, \tag{3.1}$$

$$N_{\mathrm{DATA}} = N_{\mathrm{SYM}} \times N_{\mathrm{DBPS}}, \tag{3.2}$$

$$N_{\mathrm{PAD}} = N_{\mathrm{DATA}} - (16 + 8 \times \mathrm{LENGTH} + 6), \tag{3.3}$$

where LENGTH = 250, $N_{\mathrm{DBPS}} = 48$. The calculation result of N_{PAD} is 42, which indicates 42 zero bits are padded at the end of each PLCP frame.

3.4 DATA field generation

3.4.1 Scrambler

The scrambler is used to avoid long sequences of zeros or ones in the transmitted sequence, and that is achieved by defining an initial state value of the scrambling sequence generator, compute the output of the scrambling sequence generator, and performing an XOR operation between the output and data. If there are long sequences of bits of the same value, the scrambler converts input strings into seemingly random output strings of the same length.

In our Simulink model, the scrambler uses the generator polynomial $S(x) = x_7 + x_4 + 1$ and the initial state is 1011101.

3.4.2 Convolutional encoder

Convolutional Encoder is used for error correction, which follows the industry-standard generator polynomials, $g_0 = 1011011_2$ and $g_1 = 1111001_2$. The coding rate $R = 1/2$. Figure 3.5 shows the structure of convolutional encoder for this model [1].

3.4.3 Interleaving

This part includes two-step permutation, which make the encoded bits robust to subcarriers interferences and adjacent bits loss [1]. The first and second permutations are defined by the below equations

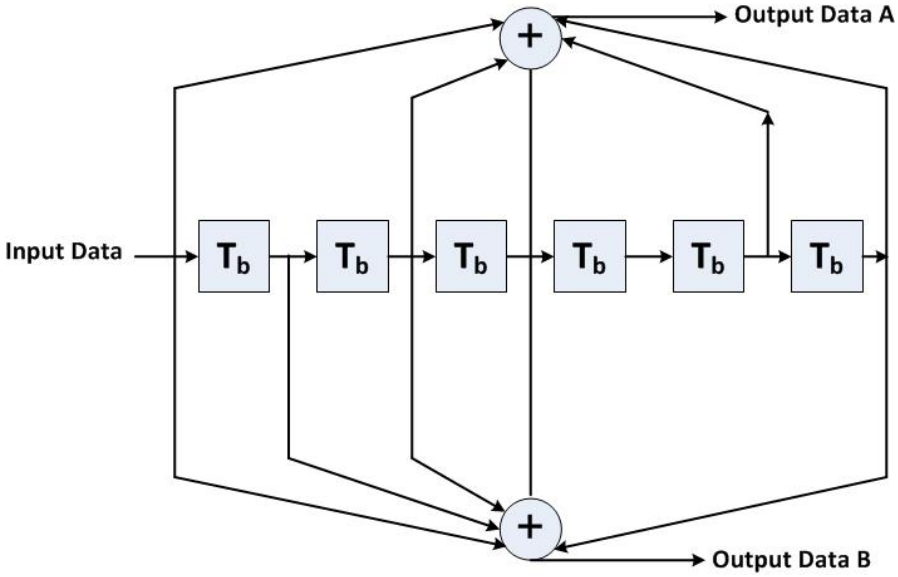

Figure 3.5: Convolutional encoder ($k = 7$)

$$\begin{aligned} i &= (N_{\text{CBPS}}/16)(k \mod 16) + \lfloor k/16 \rfloor \\ k &= 0,1,...,N_{\text{CBPS}} - 1 \end{aligned} \tag{3.4}$$

$$\begin{aligned} j &= s \times \lfloor i/s \rfloor + (i + N_{\text{CBPS}} - \lfloor 16 \times i/N_{\text{CBPS}} \rfloor) \mod s \\ i &= 0,1,...N_{\text{CBPS}} - 1, \end{aligned} \tag{3.5}$$

where subcarrier k is mapped to i, then subcarrier i is mapped to j, s is determined by N_{BPSC}, $s = \max(N_{\text{BPSC}}/2,1)$.

For the SIGNAL field, the modulation scheme is Binary Phase Shift Keying (BPSK) and the coding rate is 1/2, $N_{\text{CBPS}} = 48$, $N_{\text{BPSC}} = 1$; For the data part, the modulation scheme is QPSK and the coding rate is 1/2, $N_{\text{CBPS}} = 96$, $N_{\text{BPSC}} = 2$.

3.4.4 Subcarriers mapping

This block inserts 4 pilot subcarriers into 48 complex numbers [2], these 48 complex number are separated by 6 groups, and the below function describes how that is implemented [1]

$$M(k) = \begin{cases} k-26, & 0 \le k \le 4 \\ k-25, & 5 \le k \le 17 \\ k-24, & 18 \le k \le 23 \\ k-23, & 24 \le k \le 29 \\ k-22, & 30 \le k \le 42 \\ k-21, & 43 \le k \le 47 \end{cases} \tag{3.6}$$

$M(k)$ defines a mapping from subcarrier 0 to 47 into frequency offset index -26 to 26. The 4 pilot subcarriers and the dc subcarrier will be allocated in the 5 slots between these 6 groups.

Then 11 complex zeros are inserted at the end of index 53, there are 43 OFDM symbols in DATA part and 1 OFDM symbol in SIGNAL part, which generate a matrix of [64 x 44], where 64 is the number of subcarriers and 44 is the number of OFDM symbols.

3.4.5 IFFT

This block is to convert the transmit information from frequency domain into time domain [3], using a 64-point IFFT. In Simulink, the selector block copies subcarriers -26 to -1 into IFFT index 38 to 63, while subcarriers 1 to 26 are mapped to the same IFFT indexes. The remaining subcarriers are set to 0 [1].

3.5 Cyclic prefix

The cyclic prefix is used to avoid Inter Symbol Interference (ISI) from the previous frame. There are three kind of guard times: for short training sequence, 10 symbols can be regarded as cyclic prefix of each other, for long training sequence, the guard time is 3.2 μs, for SIGNAL and DATA field, the guard time is 1.6 μs.

The transmit signal in time and frequency domain is shown in Figure 3.6 and Figure 3.7. In Figure 3.6, each index corresponds to one sample, and the sampling time $T_s = 0.1$ μs.

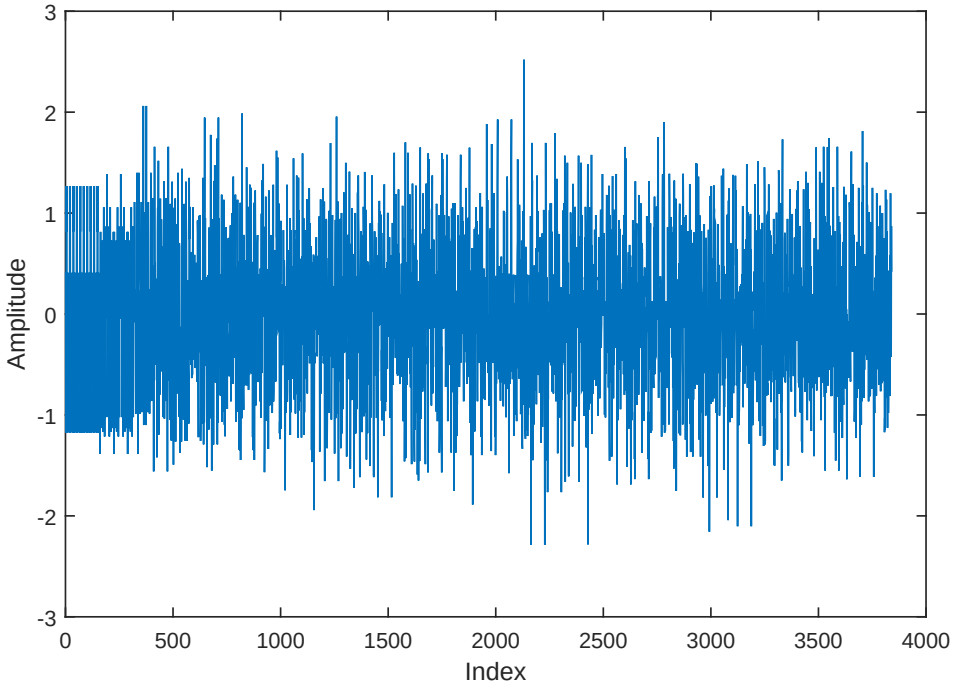

Figure 3.6: Transmit signal in time domain

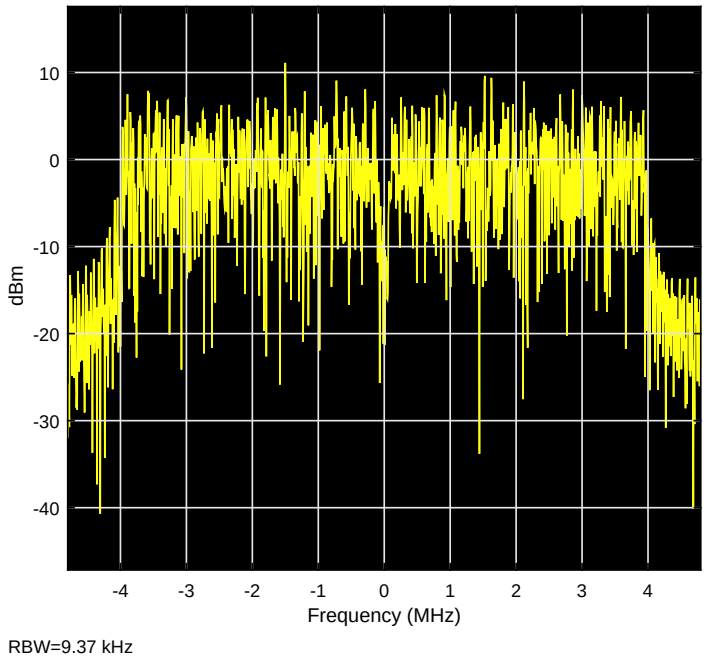

Figure 3.7: Transmit signal in frequency domain

4

The Receiver

The receiver model includes the following blocks: frame detection, symbol alignment, frequency offset detection, channel estimation and final processing block. Figure 4.1 is the block diagram in Simulink.

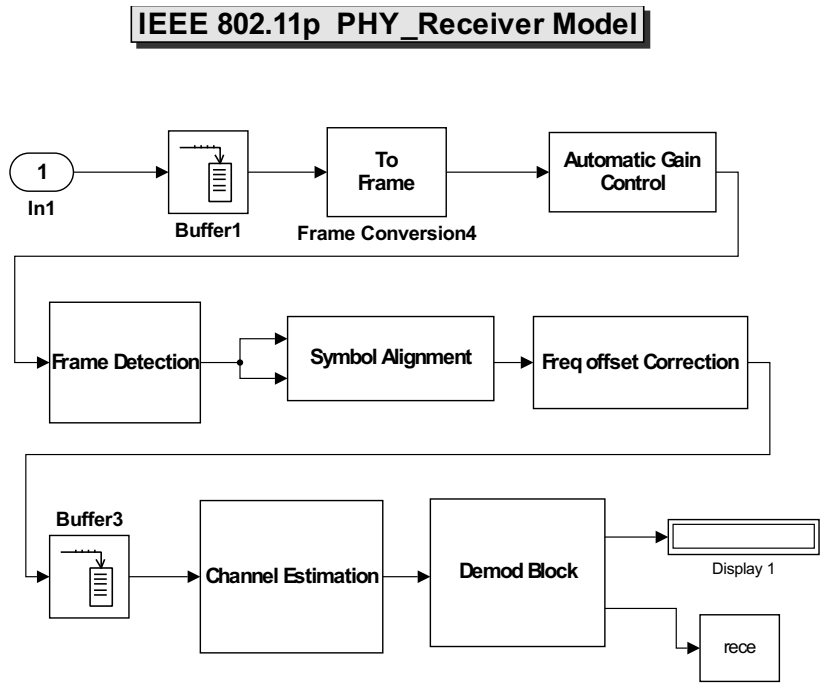

Figure 4.1: The receiver model in Simulink/Matlab

4.1 Frame detection

Frame detection is the first task implemented in the received chain. Due to the cyclic property of the short training sequence the auto correlation is high at the beginning of the frame [4]. Thus the frame detection is achieved by computing the maximum value of the correlation between the received signal and short training sequence to detect the start of a PLCP frame. The autocorrelation value of the received sample stream is calculated by three moving average filters in the model and they calculate the autocorrelation coefficients within a reasonable window. The equation below is used for the calculation of the autocorrelation [5], where $s[n]$ stands for short training sequence and $\bar{s}[n]$ stands for the complex conjugation of $s[n]$,

$$a[n] = \sum_{k=0}^{N_{\text{win1}}-1} s[n+k]\bar{s}[n+k+16]; \tag{4.1}$$

$$p[n] = \sum_{k=0}^{N_{\text{win2}}-1} s[n+k]\bar{s}[n+k]; \tag{4.2}$$

$$a_{\text{MA}}[n] = \frac{1}{N_{\text{win1}}} \sum_{k=0}^{N_{\text{win1}}-1} a[n-k]; \tag{4.3}$$

$$p_{\text{MA}}[n] = \frac{1}{N_{\text{win2}}} \sum_{k=0}^{N_{\text{win2}}-1} p[n-k]; \tag{4.4}$$

$$c[n] = \frac{|a_{\text{MA}}[n]|}{p_{\text{MA}}[n]}; \tag{4.5}$$

$$c_{\text{MA}}[n] = \frac{1}{N_{\text{win3}}} \sum_{k=0}^{N_{\text{win3}}-1} c[n-k]. \tag{4.6}$$

The purpose of using moving average filter is to suppress the noise in received signal. After several experiments, $N_{\text{win1}} = 48$, $N_{\text{win2}} = 64$ and $N_{\text{win3}} = 80$ are found to be the optimal values for the filter window sizes. The result after the correlator is depicted in Figure 4.2. Because the autocorrelation $a[n]$ is normalized as $c[n]$, the receiver detects a frame when the normalized autocorrelation peak exceeds the predefined threshold of 0.8.

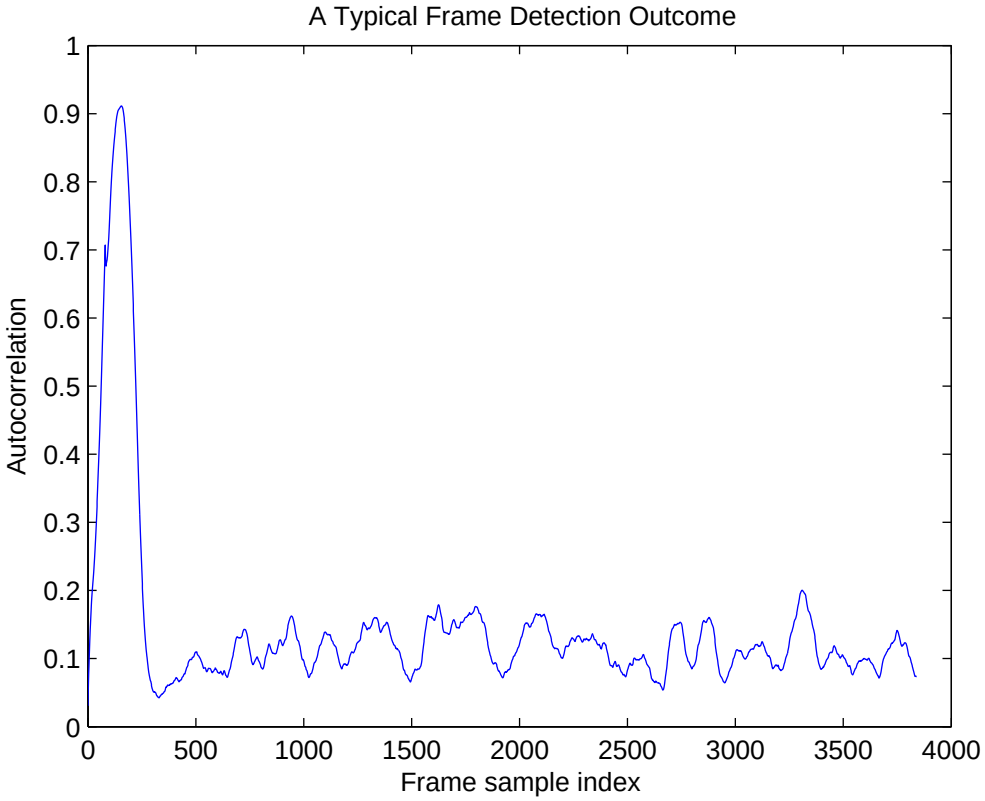

Figure 4.2: Typical results after the correlator for frame detection

4.2 Symbol alignment

The symbol alignment is based on correlating one long training symbol with the received PLCP frame [6], and this aligns the start of the data symbols. Three maximum peaks are computed. They are ordered in the increasing order of indices. Offset of 64 is added to the third one to obtain the index of the first SIGNAL symbol. This is calculated as [5]

$$N_{\mathrm{P}} = \underset{n\in\{0,\ldots,N_{\mathrm{preamble}}\}}{\arg\max_3} \sum_{k=0}^{63} s[n+k]\overline{\mathrm{LT}}[k], \tag{4.7}$$

$$n_{\mathrm{P}} = \max(N_{\mathrm{P}}) + 64. \tag{4.8}$$

The operation $\arg\max_3$ calculates the top three indices maximizing the correlation of the input with one long training symbol, thus N_{P} returns the indices of

three maximum peaks. This procedure is performed in Simulink by implementing a correlator and a sample selector [7]. There is a configurable threshold inside the selector to determine whether the peaks are from noise or signal. In Figure 4.3, the output from correlator shows the characteristic correlation property of long training symbols.

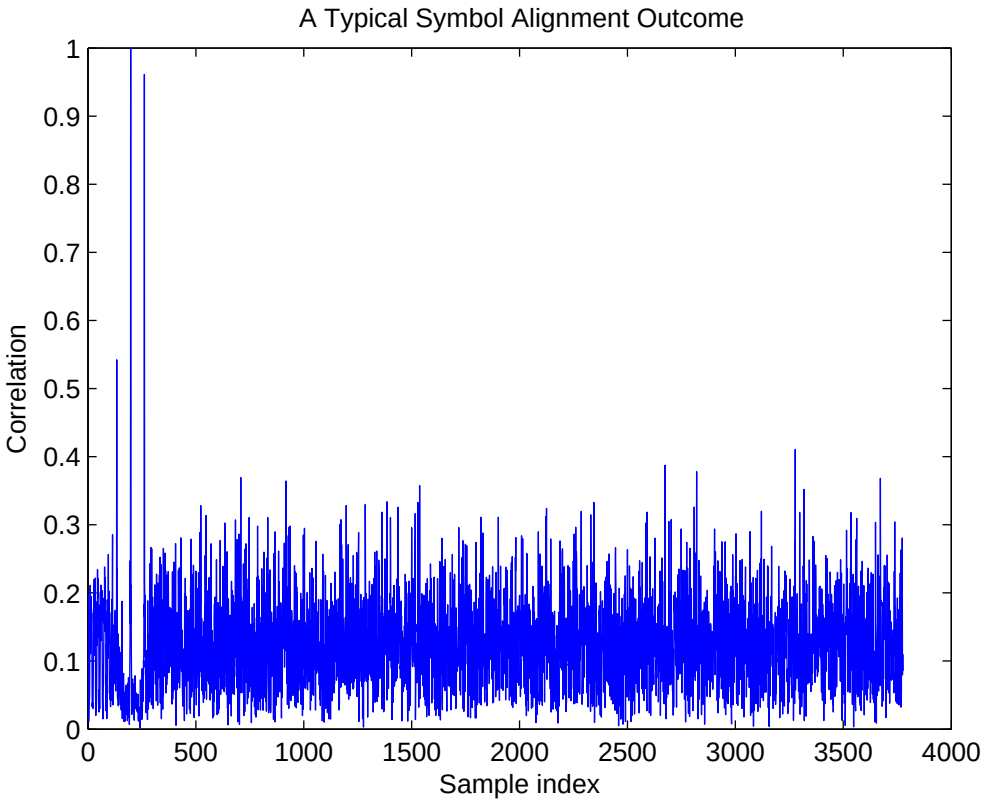

Figure 4.3: Typical results for symbol alignment

4.3 Frequency offset correction

The frequency offset correction is implemented using the cyclic property of the short training sequence, which is based on the following equation [5]

$$\mathrm{d}f = \frac{1}{16} \arg \left(\sum_{n=0}^{N_{\text{short}}-1-16} s[n]\bar{s}[n+16] \right). \tag{4.9}$$

In normal case, the short training sample $s[n]$ is equal to $s[n+16]$, and $s[n]\bar{s}[n+16]$ is a real number. If a frequency offset is introduced, $s[n]\bar{s}[n+16]$ will be a complex number. There are 16 samples in a short training symbol, which are all regarded as rotated by the frequency offset. The final offset is calculated by averaging the summation of these 16 frequency offsets.

4.4 Channel estimation

The channel estimation is implemented in frequency domain after discarding the cyclic prefix and performing FFT operation on each received OFDM symbol. The system is modeled as

$$r(k) = H(k)s(k) + n(k), \tag{4.10}$$

where $s(k)$ and $r(k)$ are the transmit and receive signals, $H(k)$ is the complex channel gain and $n(k)$ denotes the noise in frequency domain.

The received symbol $r(k)$ is a scaled and rotated version of $s(k)$ plus noise. In order to remove the channel distortion, one method is to send a known message to the receiver, which is usually called training sequence. The receiver can estimate the channel by

$$\hat{H}(k) = r(k)/s(k). \tag{4.11}$$

Then the receiver will use this information to compensate the $r(k)$. If the channel varies fast, the training symbols can be periodically repeated or decision feedback based methods have to be used.

The channel estimation block uses long training sequence to equalize the received signals [8]. The input for this block includes long training sequence and the remaining data part. At the beginning, long training sequence is extracted from the received signal and converted into frequency domain. Then this received long sequence is divided by the ideal long training, therefore the channel estimates in frequency domain are calculated. The remaining part without long training is processed with removal of OFDM symbol cyclic prefix. After FFT operation, the channel estimation is performed and the DC component is discarded. In the end, the data part gets recovered by equalizing with the channel estimate:

$$\hat{s}(k) = r(k)/\hat{H}(k). \tag{4.12}$$

4.5 Demodulation and decoding

The modulation scheme is QPSK and the data is sent repeatedly, making the SIGNAL part unchanged during the communication. After the hard QPSK demodulator and deinterleaver, a hard decision Viterbi decoder in terminated mode is used to decode the convolutionally encoded information.

The PSDU part is extracted after the descrambler block. The final block calculates the BER in each received packet and displays the decoded ASCII text on the command window. The PER is calculated as

$$\text{PER} = \frac{\text{Number of error packets}}{\text{Number of transmitted packets}}. \tag{4.13}$$

5

Simulation Model Outcomes

This chapter gives a description of the verification and interference simulation results from the established Simulink model. The interference performance was examined on the simulation model, and that was made after verifying the simulation model.

5.1 Verification

The verification procedures are configured by running the system model through an Additive White Gaussian Noise (AWGN) channel. The Signal to Noise Ratio (SNR) value in the AWGN Simulink block is modified to observe how it affects the BER in the model.

Two cases are discussed here. One is test the BER of the system over AWGN channel without convolutional coding and the other case is with convolutional coding.

For the BER of system over AWGN channel without convolutional coding, the theoretical curve is calculated by the following equation

$$P_{\mathrm{b}} = Q\left(\sqrt{2E_{\mathrm{b}}/N_0}\right) = \frac{1}{2}\operatorname{erfc}(\sqrt{E_{\mathrm{b}}/N_0}), \tag{5.1}$$

where E_{b} is the signal energy associated with each data bit, $N_0/2$ is the noise spectral density, E_{b}/N_0 is the SNR/bit.

For the BER of system over AWGN channel with hard decision convolutional coding, the bit error probability upper bound is calculated with bercoding function in Matlab.

In the test, 10000 packets are transmitted to get each BER sample for each E_b/N_0 value. We plot BER versus E_b/N_0 and results are shown in Figure 5.1. When the convolutional coding and decoding blocks are removed from system, the simulation curve follows the theoretical curve with small deviation. In the other case, when the system is complete, the curve is verfied by comparing with the theoretical upper bound, which proves that the system meets the theoretial requirements.

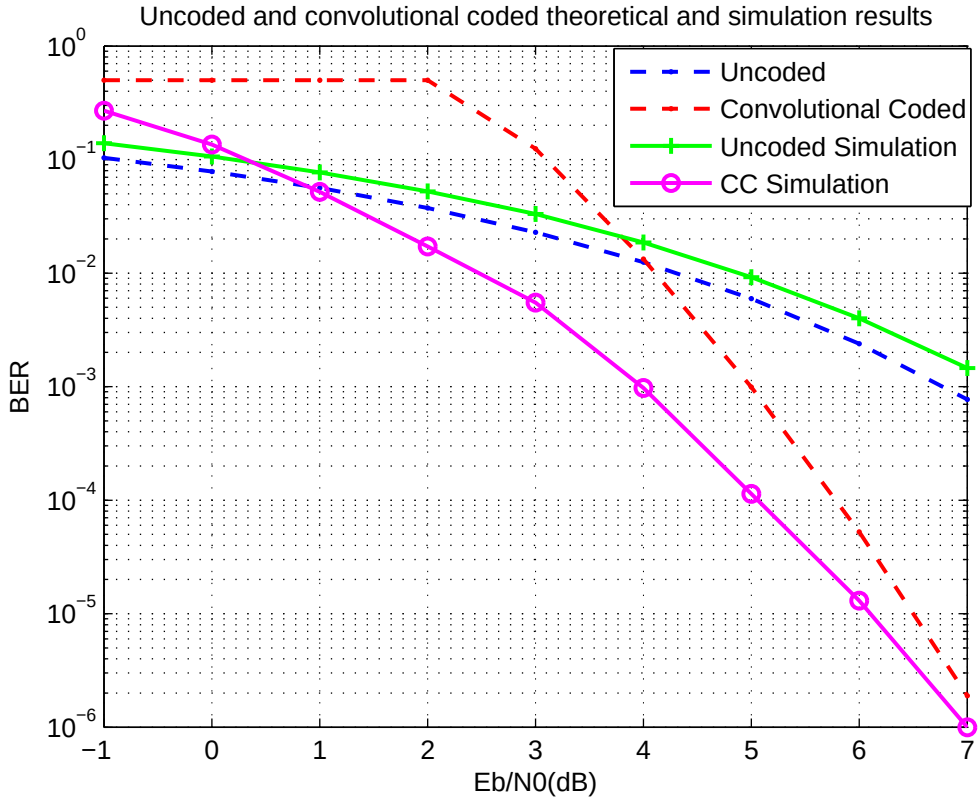

Figure 5.1: Theoretical and simulation results

The model is verified by checking the results with the theoretical BER versus E_b/N_0 curve. The next step is to insert the interference signals to the transmitted signal under fixed SNR and observe the effect on the PER and BER with different signal to interference levels.

5.2 The intermediate channel

The intermediate channel part is used to introduce fading, noise and different interference signals. The interference signal types are provided by Volvo Cars and are added to the transmitted signal. The description and the results are explained in the sections below.

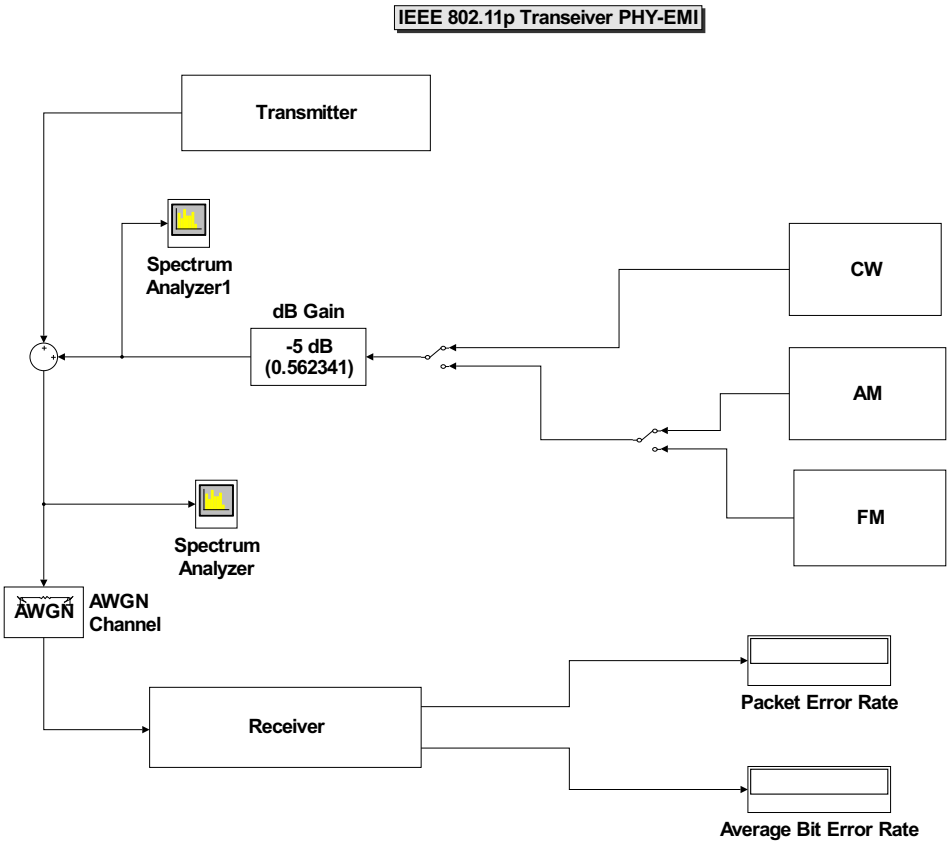

Figure 5.2: Diagram showing the measurement setup with AWGN and Interference signal blocks

5.2.1 Interference signals

In this thesis work we inserted three types of interference signals. Each of these interferences are analyzed and the BER, PER, Signal to Interference Ratio (SIR) are calculated to show how these interferences affect the 802.11p system performance. For each test, 2000 packets are transmitted.

5.2.2 Continuous wave

The CW wave interference is introduced to the system and the equation below shows the mathematical expression

$$s(t) = A_{\mathrm{c}}\sin(2\pi f_{\mathrm{c}}t + \varphi), \tag{5.2}$$

where A_{c} is the amplitude, f_{c} is the carrier frequency and φ is the phase.

In the model, $A_{\mathrm{c}} = 1$. In order to compare the effects of interferences located in different frequency bands, both for low band and high band, f_{c} is modified by three frequencies: 1 MHz, 2 MHz and 3 MHz.

Figure 5.3 and Figure 5.4 show the spectrum of the CW signal at 1 MHz and the corresponding 802.11p signal spectrum. The position the CW spectrum depends on the carrier frequency. The BER and PER test results over 2000 packets are depicted in Figure 5.5 and Figure 5.6. The simulations are performed by fixing the power of transmitted signal and AWGN with SNR of 10 dB, and increasing the power of interference signal by 1 dB after every 2000 packets are transmitted, meanwhile a measuring block tracks the resulting SIR values. The SIR is defined as

$$\mathrm{SIR} = 10\log_{10}\left(\frac{S}{I}\right), \tag{5.3}$$

where S is the power of signal and I is the power of interference.

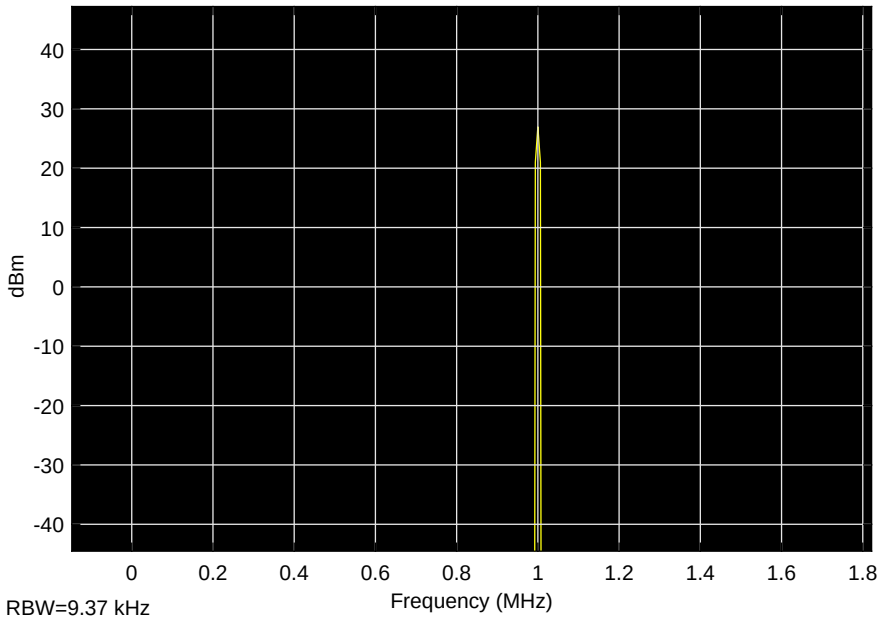

Figure 5.3: Spectrum of CW at 1 MHz

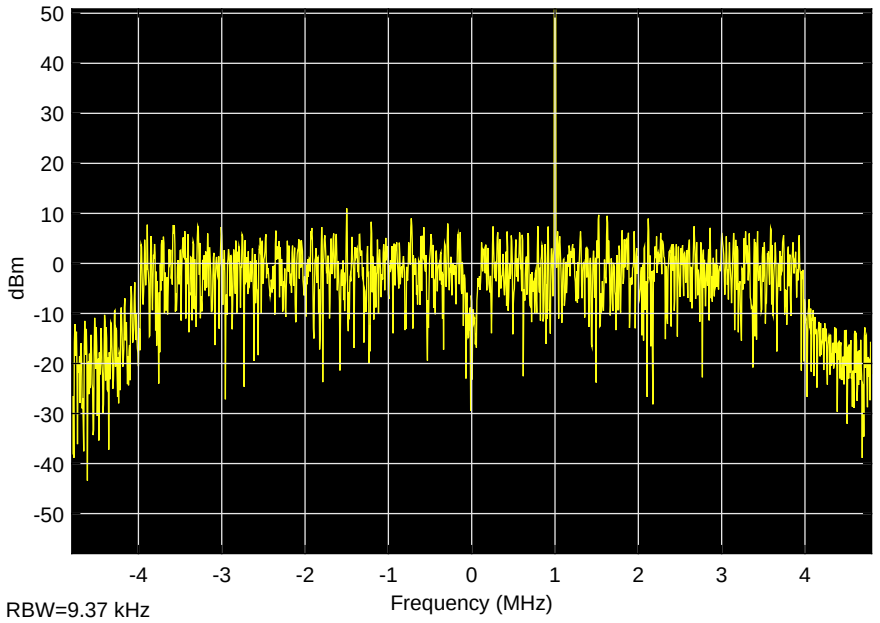

Figure 5.4: Spectrum of signal with CW at 1 MHz

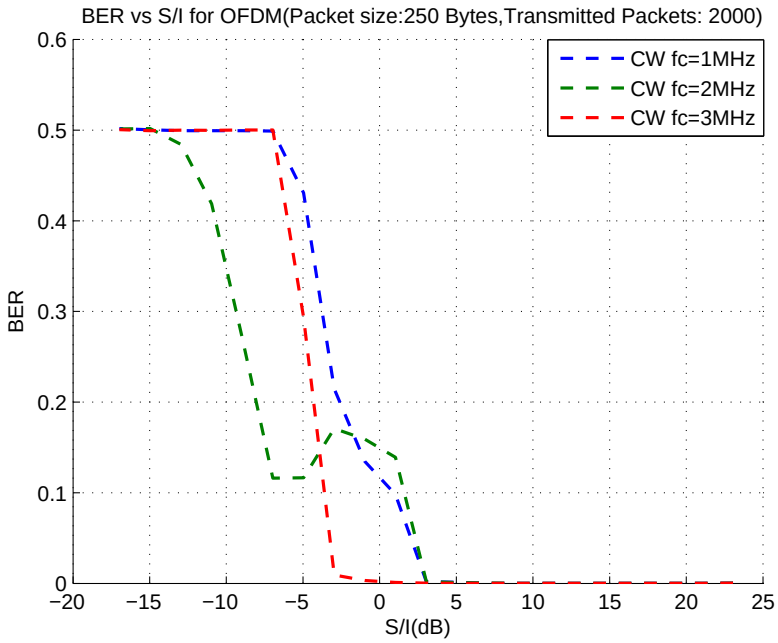

Figure 5.5: BER vs SIR in AWGN with CW

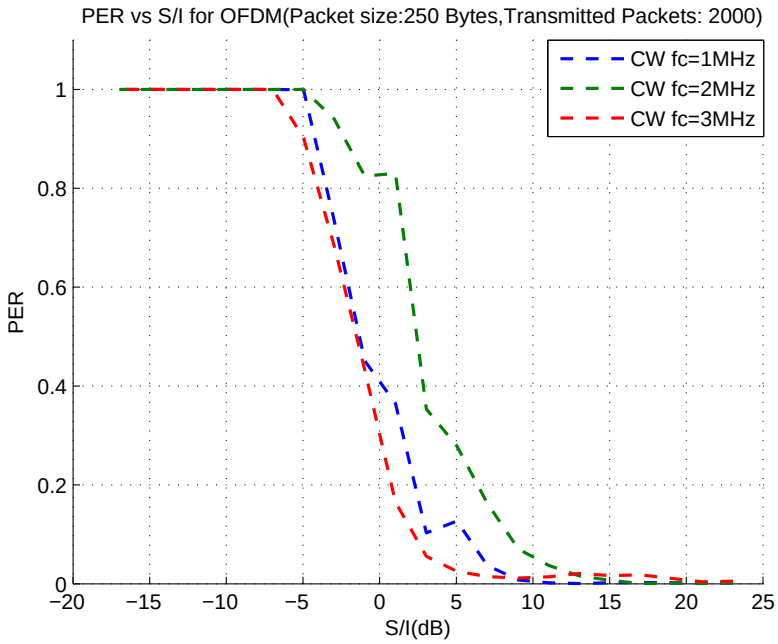

Figure 5.6: PER vs SIR in AWGN with CW

Figure 5.5 shows the BER performance and at the 1 MHz and 3 MHz looks good, while the 2 MHz performance looks strange and the optimal plot is at 3 MHz. Figure 5.6 for the PER performance gives almost the same result with a distorted curve at 2 MHz. The result shows that the system does not work properly at 2 MHz.

At the carrier frequency 2 MHz, we notice that there is a fluctuation. The reason for this behavior has not been found and further investigation is required. Due to the imperfection of the receiver model, the receiver model might also need more work to be reliable.

From the results of PER, it can be seen that the carrier frequencies of the CW interference have an impact upon the performance of the system.

5.2.3 AM wave

The AM wave interference is introduced in this part to the system and the equation below shows the mathematical expression

$$s(t) = [A_\mathrm{c} + M\cos(2\pi f_\mathrm{m} t + \phi)]\cos(2\pi f_\mathrm{c} t), \tag{5.4}$$

where M is the modulation amplitude, f_m is the modulation frequency and ϕ is the phase of modulation signal. The modulation index is defined as the ratio

$$m = \frac{M}{A_\mathrm{c}} \, . \tag{5.5}$$

In the simulation, The modulation index $m = 80\%$, $f_\mathrm{c} = 1$ MHz and 3 MHz, $f_\mathrm{m} = 5$ kHz, 20 kHz and 50 kHz.

In order to determine the frequencies contained in the AM interference, the modulated part of AM can be rewritten as

$$s(t) = A_\mathrm{c}\cos(2\pi f_\mathrm{c} t) + \frac{A_\mathrm{c} M}{2}\left[\sin(2\pi(f_\mathrm{c} + f_\mathrm{m})t) + \sin(2\pi(-f_\mathrm{c} + f_\mathrm{m})t)\right]. \tag{5.6}$$

In Figure 5.7 and Figure 5.8, the spectrum of AM 80%, $f_\mathrm{m} = 50$ kHz with $f_\mathrm{c} = 1$ MHz and the received 802.11p frame are shown.

Figure 5.9 and Figure 5.10 show the simulation results of BER and PER with AM interference over 2000 packets. In this simulation, the SNR is fixed at 10 dB and the powers of the interference signal is increased by 1 dB after every 2000 packets, the corresponding SIR is also calculated.

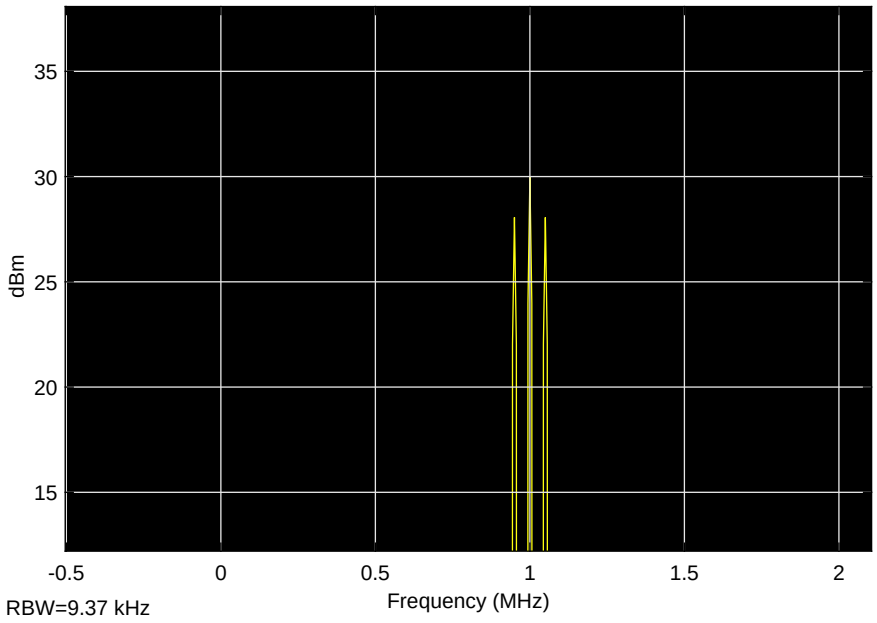

Figure 5.7: Spectrum of AM $f_{\mathrm{m}} = 50$ kHz at 1 MHz

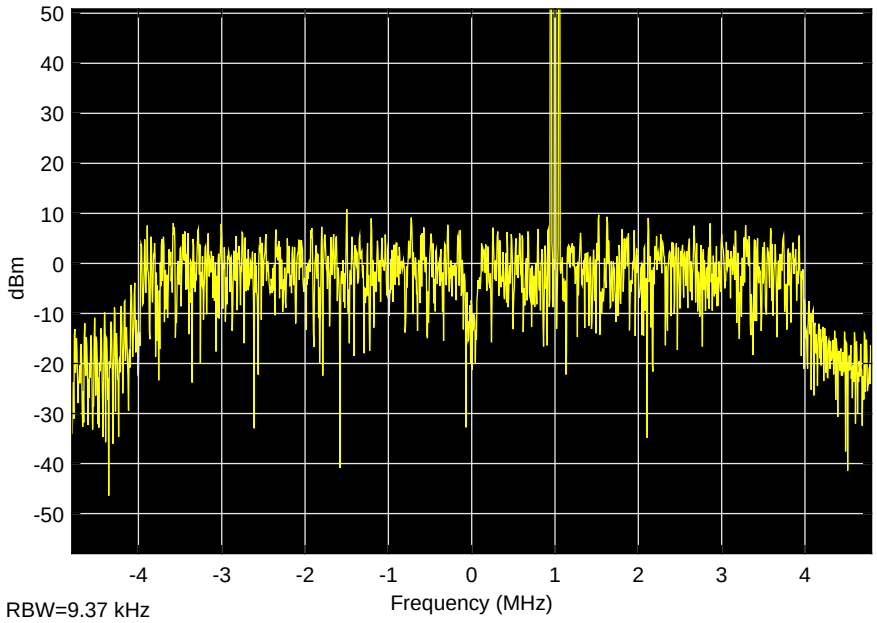

Figure 5.8: Spectrum of signal with AM $f_{\mathrm{m}} = 50$ kHz at 1 MHz

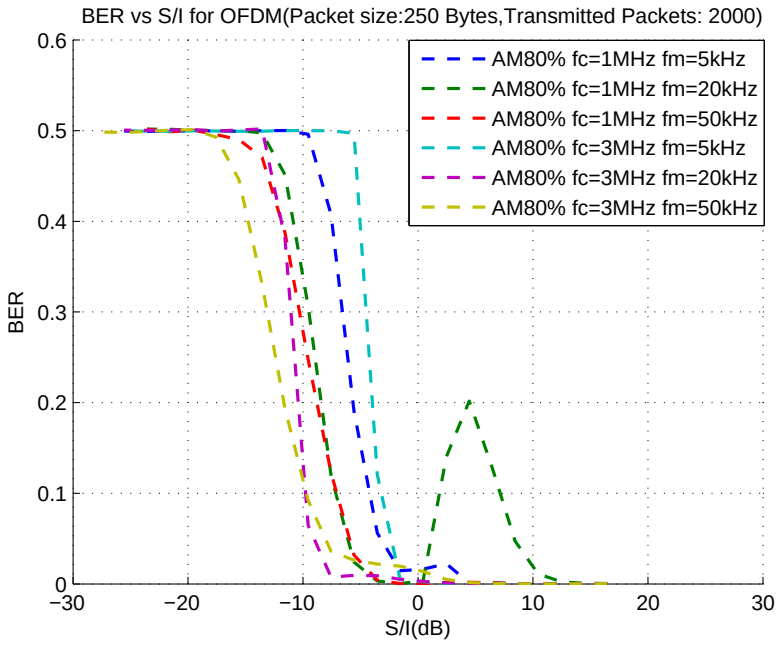

Figure 5.9: BER vs SIR in AWGN with AM

For the AM wave interference, we plotted BER and PER versus SIR by fixing the modulation index to 80% and choosing two carrier frequencies 1 MHz and 3 MHz, each was tested over three different modulation frequencies 5 kHz, 20 kHz and 50 kHz. The plot shows the result for BER versus SIR in Figure 5.9, which depicts the curves with monotonically decreasing parts at high carrier frequencies, while at low carrier frequencies a significant fluctuation can be seen at $f_c = 1$ MHz, and $f_m = 20$ kHz.

In Figure 5.10, we notice the curves of PER versus the SIR looks fluctuant especially with $f_m = 20$ kHz at $f_c = 1$ MHz and 3 MHz. We have not been able to find the reason for this behavior and more work is needed.

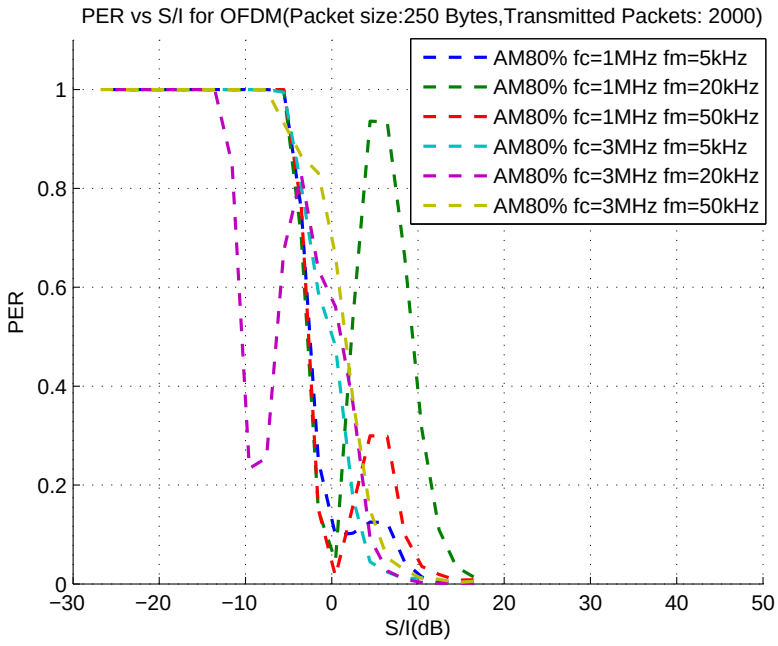

Figure 5.10: PER vs SIR in AWGN with AM

5.2.4 FM wave

FM wave interference is introduced in this part to the system and the equation below shows the mathematical expression

$$s(t) = A_{\mathrm{c}}\cos\left(2\pi f_{\mathrm{c}}t + 2\pi k_{\mathrm{f}}\int_0^t m(\tau)\,\mathrm{d}\tau\right). \tag{5.7}$$

where k_{f} is the frequency deviation, $m(t)$ is the modulation signal $A_{\mathrm{m}}\cos(2\pi f_{\mathrm{m}}t)$.

In the simulation, $f_{\mathrm{c}} = 1$ MHz and 3 MHz to verify the system performance in both low band and high band, $f_{\mathrm{m}} = 5$ kHz, 20 kHz and 50 kHz, frequency deviation = 100 kHz and 300 kHz. The modulation index is expressed as

$$\beta = \Delta f_{\mathrm{p}}/f_{\mathrm{m}}, \tag{5.8}$$

Δf_{p} = peak frequency deviation, and f_{m} = modulation frequency. Δf_{p} is expressed as $\Delta f_{\mathrm{p}} = k_{\mathrm{f}}A_{\mathrm{m}}$.

In the mathematical treatment, the FM signal modulated using a single sinusoid is given as [9]

$$s(t) = A_{\mathrm{c}} \sum_{n=-\infty}^{\infty} J_n(\beta)\cos(2\pi(f_{\mathrm{c}} + nf_{\mathrm{m}})t), \tag{5.9}$$

thus after Fourier transform the frequency spectrum of this FM signal equals

$$S(f) = \frac{A_{\mathrm{c}}}{2} \sum_{n=-\infty}^{\infty} J_n(\beta)[\delta(f - nf_{\mathrm{m}} - f_{\mathrm{c}}) + \delta(f + nf_{\mathrm{m}} + f_{\mathrm{c}})], \tag{5.10}$$

where the J_n is the n-th order Bessel function of the first kind. In the model, we use the first kind Bessel function up to 4th order to represent the carrier and sideband amplitudes of the FM signal.

Figure 5.11 and Figure 5.12 show the interference within the spectrum. Figure 5.13, Figure 5.14, Figure 5.15 and Figure 5.16 show the test results of BER and PER over 2000 packets. These results are obtained by fixing the power of transmitted signal and AWGN thus SNR is 10 dB, and increasing the power of interference signal by 1 dB after every 2000 packets, SIR is also calculated at the same time.

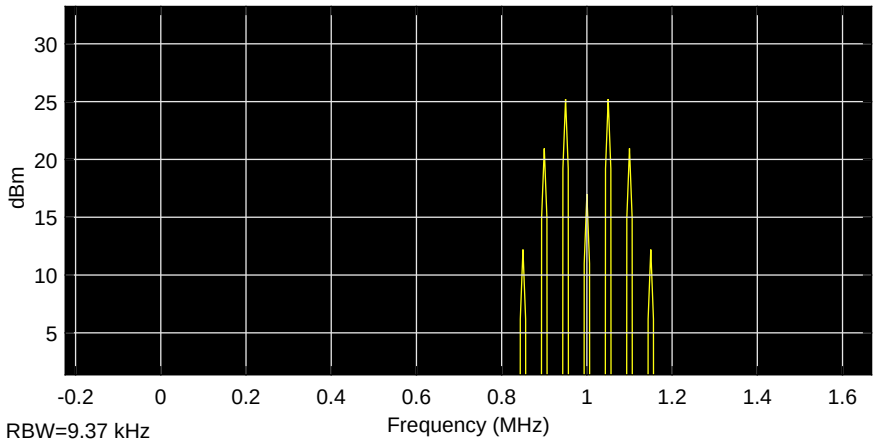

Figure 5.11: Spectrum of FM $f_{\mathrm{m}} = 50$ kHz at 1 MHz

For FM interference, deviation frequencies 100 kHz and 300 kHz with carrier frequencies 1 MHz, and 3 MHz were tested over three modulation frequencies 5 kHz, 20 kHz, and 50 kHz. In Figure 5.13 and Figure 5.14 we can see monotonically decreasing curves at all frequencies except at $f_{\mathrm{c}} = 1$ MHz, $f_{\mathrm{m}} = 20$ kHz, the

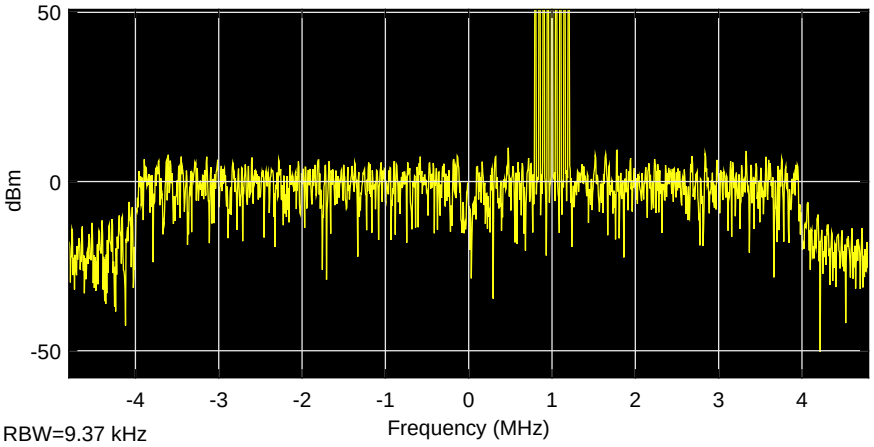

Figure 5.12: Spectrum of signal with FM $f_{\mathrm{m}} = 50$ kHz at 1 MHz

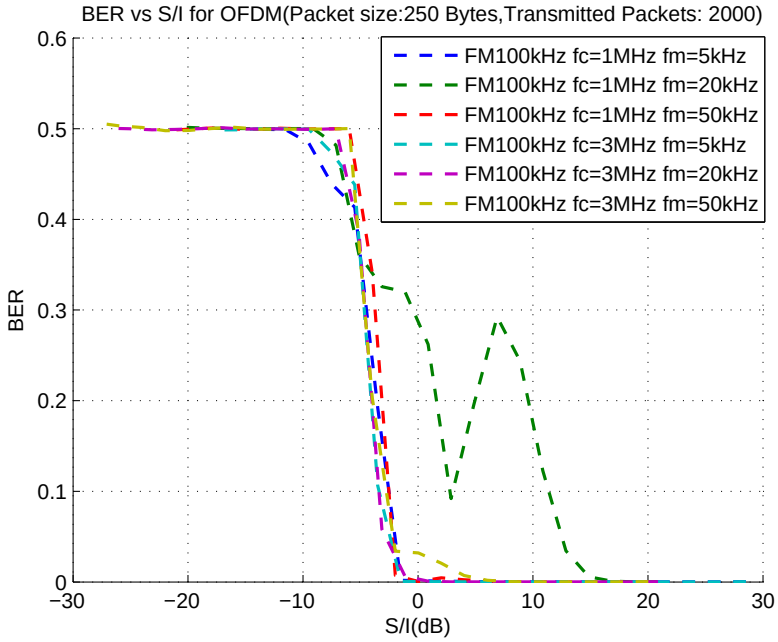

Figure 5.13: BER vs SIR in AWGN with 100 kHz deviation FM

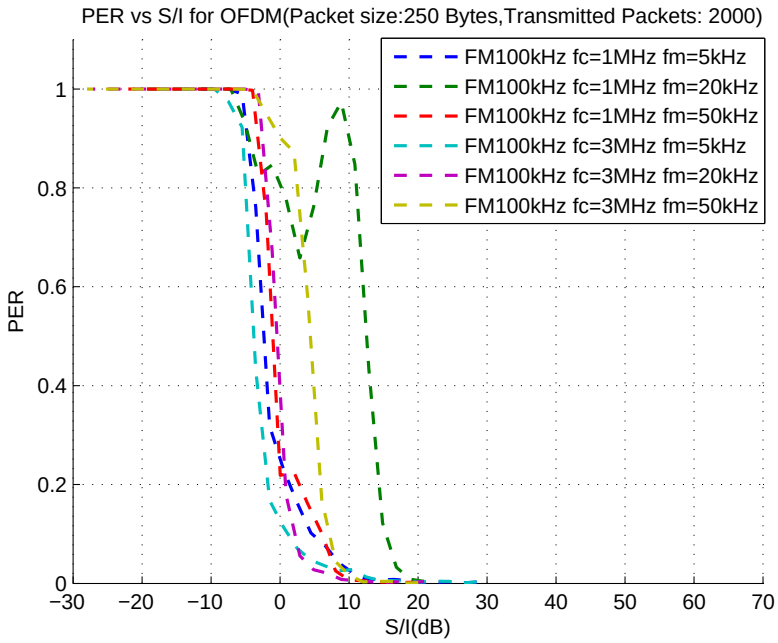

Figure 5.14: PER vs SIR in AWGN with 100 kHz deviation FM

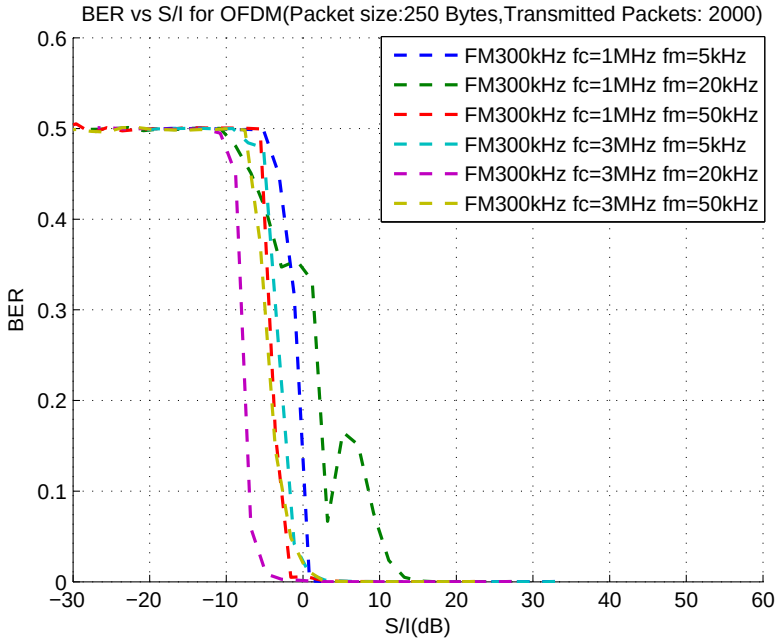

Figure 5.15: BER vs SIR in AWGN with 300 kHz deviation FM

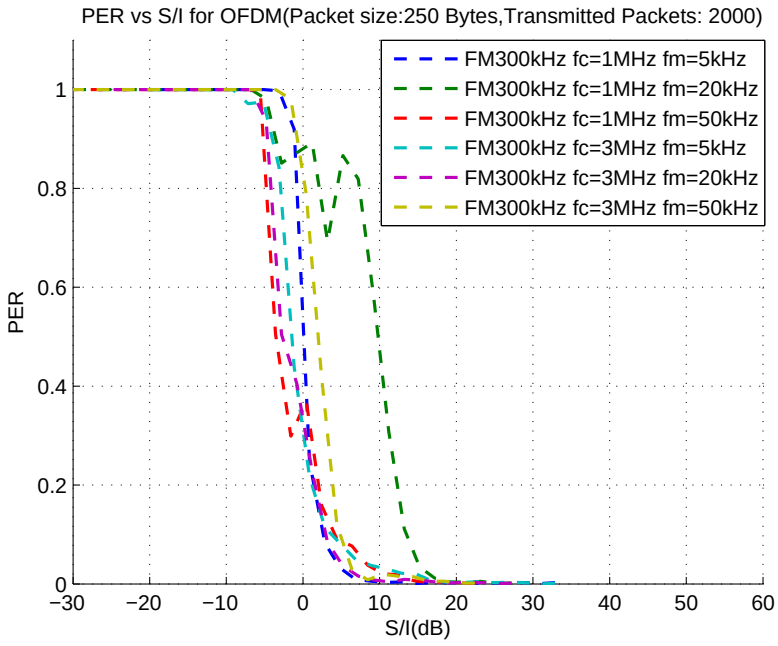

Figure 5.16: PER vs SIR in AWGN with 300 kHz deviation FM

fluctuant curves from this combination can also be seen in Figure 5.15 and Figure 5.16. The FM interferences with different parameters cause similar BER and PER outcomes.

From the spectrum we can see that FM wave has a wider spectrum span than AM wave, which means that the increase of FM signal power will simultaneously affect more adjacent subcarriers at some interference signal strength levels. By comparing Figure 5.10, Figure 5.14 and Figure 5.16, we can see the PER performance near 0 dB SIR degrades more in case of AM than FM.

6

Conclusions and Future Work

6.1 Conclusions

This thesis work is focused on developing and verifying a simulation model of the IEEE 802.11p transceiver in Simulink. The Simulink model is able to reproduce theoretical results for the AWGN channel fairly well, as seen in Figure 5.1. Hence, the model is verified for use over the AWGN channel, which gives some confidence for its correctness also for interference channels.

The next task in this thesis work is the observation of the effect of the interference on the system, which is implemented by inserting different types of interference signals and each interference is observed in the transmitted spectrum. The model test procedures are based on inserting the interference signals to the model and observing the behavior by plotting the BER versus SIR and PER versus SIR for 2000 packet each time. Various combinations of amplitudes and frequencies give a distinct view about how the interferences affect the whole system. More work and analysis is needed to explain the non monotonic behavior of the BER and PER curves in case of some specific AM and FM signals in Chapter 5.

The model shows variable susceptibilities under three kinds of interferences and also under equivalent modulation scheme interference with different carrier frequencies, which means that the interference frequency located in the low band and high band have different impacts on the system.

In our model, the SIGNAL field in the PLCP frame is fixed and the receiver does not use the SIGNAL field in the model for decoding. According to the IEEE 802.11p standard, when the SIGNAL field is corrupted the whole PLCP frame should be discarded, which means the receiver model can be improved for better performance.

Finally, we conclude that this model is a generic model that can be widely used for different purposes by replacing interference sources to test the stability of the IEEE 802.11p compliant communication system.

6.2 Future work

We have tried to run the simulated model on real hardware by using two USRP devices from Ettus type N210. That was done by separating the simulated model into two parts, one part for the transmitter and the other part for the receiver. Once these models are separated we run them on two computers by inserting the USRP hardware blocks in Simulink for each of the model parts and inserted the frequency 5.9 GHz to match the standard frequency range. Figure 6.1 shows the diagram of the hardware connection.

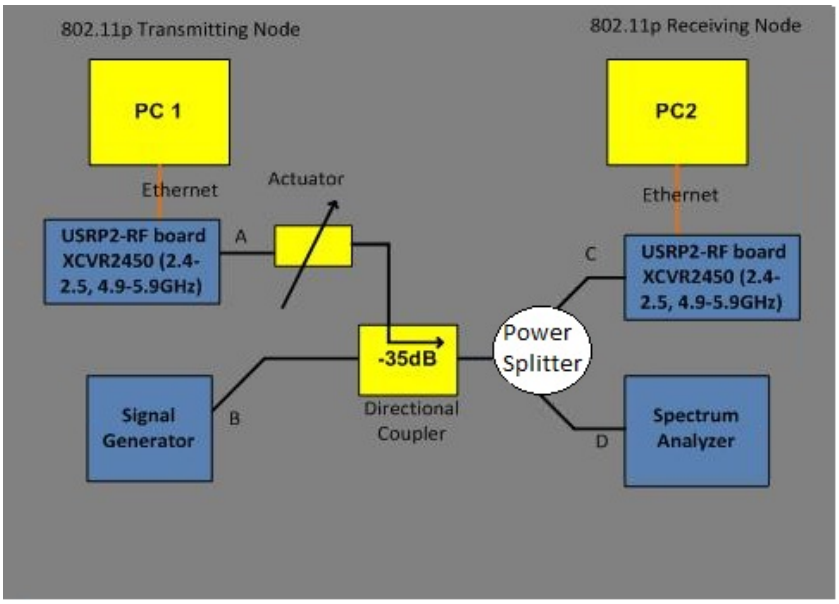

Figure 6.1: The USRP board interconnection between the computer (model/Simulink) and the RF (Antenna or cable)

The hardware system setup is based on two computers, and two USRP's (Universal Software defined Radio), Figure 6.2 shows the implemented hardware setup overview.

The main goal was to test the models on the USRP hardware and to insert a real interference signal and observe the effect on the BER with QPSK modulation scheme. That was not achieved in this thesis work because of the uncertainty of the hardware. Due to time constraints, only the software modulation model was achieved.

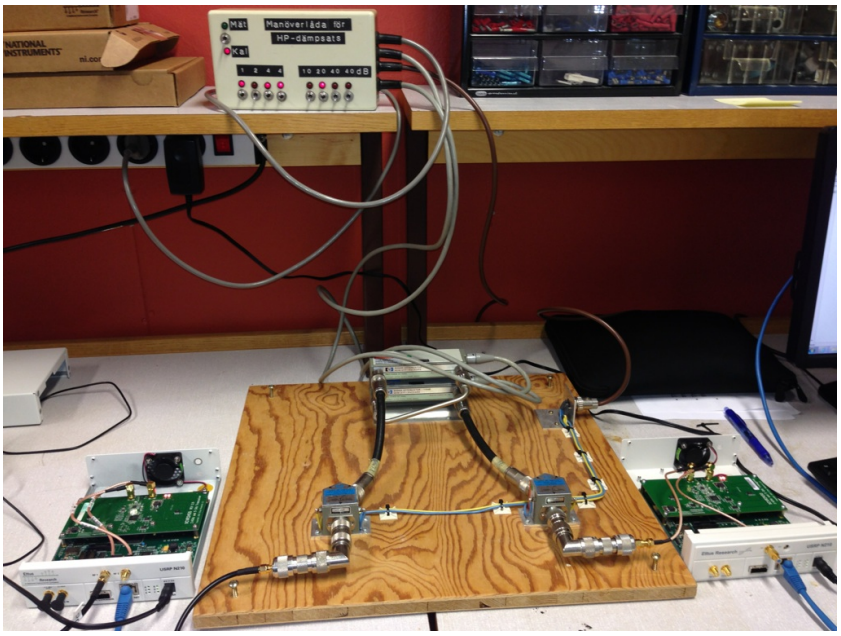

Figure 6.2: The real hardware picture setup

The hardware setup also includes an attenuator, directional coupler, and a signal generator used to generate the interference signal to the channel. On the receiver side a spectrum analyzer is used to observe the behavior of the received signal.

Each model runs on a separate computer, the software used is Simulink/Matlab and each computer is connected to an USRP via Ethernet cable. The two USRP's are connected together by a cable through an attenuator which attenuates the power with 30dB.

The future work can be made on implementing the model on real hardware such as USRP, which means that the model shall be separated into two parts. The transmitter and the receiver shall run on different computers connected with USRP for sending and receiving the packets. The model also needs to be improved if it is utilized with hardware.

Bibliography

[1] IEEE Standard for Information technology–Telecommunications and information exchange between systems local and metropolitan area networks–Specific requirements Part 11: Wireless LAN Medium Access Control (MAC) and Physical Layer (PHY) Specifications, IEEE Std 802.11-2012 (Revision of IEEE Std 802.11-2007) (2012) 1–2793.

[2] P. Fuxjäger, A. Costantini, D. Valerio, P. Castiglione, G. Zacheo, T. Zemen, F. Ricciato, IEEE 802.11 p transmission using GNURadio, in: 6th Karlsruhe Workshop on Software Radios (WSR), Citeseer, 2010, pp. 1–4.

[3] M. Rahman, S. Latif, T. Ahad, P. K. Dey, M. Rabbi Ur Rashid, B. Rashid, S. Ahmed, The study of OFDM ICI cancellation schemes in 2.4 GHz frequency band using software defined radio, in: Wireless Communications, Networking and Mobile Computing (WiCOM), 2011 7th IEEE International Conference, 2011, pp. 1–6.

[4] C.-H. Liu, On the design of OFDM signal detection algorithms for hardware implementation, in: IEEE Global Telecommunications Conference, 2003. GLOBECOM'03., Vol. 2, 2003, pp. 596–599.

[5] B. Bloessl, M. Segata, C. Sommer, F. Dressler, An IEEE 802.11 a/g/p OFDM receiver for GNU radio, in: Proceedings of the second workshop on Software radio implementation forum, ACM, 2013, pp. 9–16.

[6] M. Tichy, K. Ulovec, OFDM system implementation using a USRP unit for testing purposes, in: Radioelektronika (RADIOELEKTRONIKA), 2012 22nd International Conference, IEEE, 2012, pp. 1–4.

[7] O. Ozdemir, R. Hamila, N. Al-Dhahir, A USRP-based experimental testbed for OFDM systems impaired by I/Q imbalance, in: GCC Conference and Exhibition (GCC), 2013 7th IEEE, 2013, pp. 98–102.

[8] G. Berardinelli, P. Zetterberg, O. Tonelli, A. F. Cattoni, T. Sorensen, P. Mogensen, An SDR architecture for OFDM transmission over USRP2 boards, in: Signals, Systems and Computers (ASILOMAR), IEEE Conference Record of the Forty Fifth Asilomar Conference on, 2011, pp. 965–969.

[9] L. Der, Frequency modulation (FM) tutorial, Silicon Laboratories Inc. `http://www.silabs.com/Marcom%20Documents/Resources/FMTutorial.pdf`, [Online; accessed 17-December-2014] (2008).